

---

## Abstract

*Keywords:*

---

### 1. Introduction

The first direct evidence for point-like constituents in the nucleons came from the discovery of scaling phenomenon in Deep-Inelastic Scattering (DIS) experiments at SLAC. Enormous experimental and theoretical efforts have been devoted to the extraction and understanding of the various parton distribution functions (PDFs) in the nucleons. Electroweak processes such as DIS and lepton-pair production provide the cleanest means to extract information on the PDFs. The excellent agreement between the theory and data on the scaling-violation behavior of the PDFs has provided one of the most stringent tests for QCD as the theory of strong interaction.

During the past two decades, many important new developments related to the study of PDFs have taken place. On the theoretical side, the existence of many novel PDFs which can be extracted experimentally has been pointed out. In addition to the well studied unpolarized PDFs and the helicity-dependent PDFs, several transverse-spin and/or transverse-momentum dependent PDFs are shown to exist, and their salient features have been calculated using various theoretical models. In particular, the advent of the Lattice Gauge Theory (LGT) in calculating moments of various novel PDFs allows direct comparison between the experimental data with such first-principle QCD calculations. Specific experimental tools for probing these novel PDFs have also been suggested.

On the experimental side, the extensive measurements of polarized DIS using polarized electron and muon beams on polarized targets, as well as the detection of hadrons in coincidence with the scattered charged leptons in the Semi-Inclusive DIS (SIDIS) experiments, have allowed the first observation and extraction of several novel parton distributions. More recently, the prospect of using polarized hadronic beam colliding with possibly polarized beam/target has attracted much attention. Such measurements could

be pursued in existing facility such as the polarized p-p collider at RHIC, as well as in other hadron machines. The novel PDFs obtained in hadron collisions are expected to provide complementary and often unique information not accessible using the leptonic beams.

In the review article, we focus on the recent progress and future prospect on using hadronic beams to explore the novel parton distributions in the nucleons. In particular, we examine the unique features of the lepton-pair production (the Drell-Yan process) in hadron collision in extracting the spin and flavor dependences of PDFs.

## 2. PDF and Drell-Yan Production

### 2.1. Brief history of Drell-Yan

### 2.2. Recent Results from Drell-Yan

#### 2.2.1. Sea-quark flavor asymmetry

The earliest parton models assumed that the proton sea was flavor symmetric, even though the valence quark distributions are clearly flavor asymmetric. The flavor symmetry assumption was not based on any known physics, and it remained to be tested by experiments. Neutrino-induced charm production experiments [2] showed that the strange-quark content of the nucleon is only about half of the up or down sea quarks. Such flavor asymmetry is attributed to the much heavier strange-quark mass compared to the up and down quarks. The similar masses for the up and down quarks suggest that the nucleon sea should be nearly up-down symmetric.

The issue of the equality of  $\bar{u}$  and  $\bar{d}$  was first encountered in measurements of the Gottfried integral [3], given as

$$I_G = \int_0^1 [F_2^p(x) - F_2^n(x)] / x dx = \frac{1}{3} + \frac{2}{3} \int_0^1 [\bar{u}_p(x) - \bar{d}_p(x)] dx, \quad (1)$$

where  $F_2^p$  and  $F_2^n$  are the proton and neutron structure functions measured in DIS experiments. The second step in Eq. 1 follows from the assumption of charge symmetry (CS) at the partonic level, namely,  $u_p(x) = d_n(x)$ ,  $d_p(x) = u_n(x)$ ,  $\bar{u}_p(x) = \bar{d}_n(x)$ , and  $\bar{u}_n(x) = \bar{d}_p(x)$ . Under the assumption of a  $\bar{u}$ ,  $\bar{d}$  flavor-symmetric sea in the nucleon, the Gottfried Sum Rule (GSR) [3],  $I_G = 1/3$ , is obtained. The most accurate test of the GSR was reported by the New Muon Collaboration (NMC) [4], which determined the Gottfried integral to be  $0.235 \pm 0.026$ , significantly below  $1/3$ . This surprising result

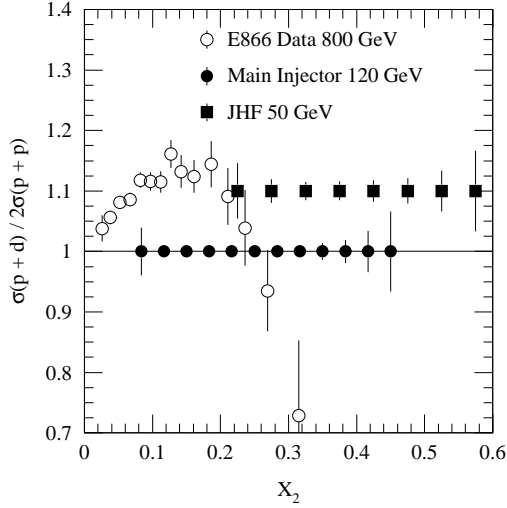


Figure 1: Data from E866 and projected sensitivities for future experiments at 50 and 120 GeV.

has generated much interest. Although the violation of the GSR can be explained by assuming unusual behavior of the parton distributions at very small  $x$ , a more natural explanation is to abandon the assumption  $\bar{u} = \bar{d}$ .

The proton-induced Drell-Yan (DY) process provides an independent means to probe the flavor asymmetry of the nucleon sea. An important advantage of the DY process is that the  $x$  dependence of  $\bar{d}/\bar{u}$  asymmetry can be determined. At Fermilab, the E866/NuSea [43, 6, 7] Collaboration measured the DY cross section ratios for  $p + d$  to that of  $p + p$  using 800 GeV proton beams. At forward rapidity region and assuming the validity of charge symmetry, one obtains

$$\sigma_{DY}(p + d)/2\sigma_{DY}(p + p) \simeq [1 + \bar{d}(x)/\bar{u}(x)] / 2. \quad (2)$$

As shown in Fig. 1, this ratio was found to be significantly different from unity for  $0.015 < x < 0.35$ , indicating an excess of  $\bar{d}$  with respect to  $\bar{u}$  over an appreciable range in  $x$ .

Many theoretical models, including meson-cloud model, chiral-quark model, Pauli-blocking model, instanton model, chiral-quark soliton model, and statistical model, have been proposed to explain the  $\bar{d}/\bar{u}$  asymmetry. Details of these various models can be found in some review articles [8, 9]. The most straightforward of these models are those that attribute the asymme-

try to the existence of a “pion cloud” in the proton. The relevance of pion cloud for sea-quark distributions appears to have first been made by Thomas in a publication [10] treating SU(3) symmetry breaking in the nucleon sea. Sullivan [11] had earlier shown that virtual meson-baryon states directly contribute to the nucleon’s structure function. More specifically, the proton is taken to a linear combination of a “bare” proton plus pion-nucleon and pion-delta states, as below,

$$\begin{aligned}
|p\rangle \rightarrow & \sqrt{1-a-b}|p_0\rangle + \sqrt{a}\left(-\sqrt{\frac{1}{3}}|p_0\pi^0\rangle + \sqrt{\frac{2}{3}}|n_0\pi^+\rangle\right) + \\
& \sqrt{b}\left(\sqrt{\frac{1}{2}}|\Delta_0^{++}\pi^-\rangle - \sqrt{\frac{1}{3}}|\Delta_0^+\pi^0\rangle + \sqrt{\frac{1}{6}}|\Delta_0^0\pi^+\rangle\right). \quad (3)
\end{aligned}$$

The subscript zeros on the virtual baryon states indicate that they are assumed to have symmetric seas, so the asymmetry in the antiquarks must be generated from the pion valence distribution. The coefficients  $a$  and  $b$  are the fractions of the  $\pi N$  and  $\pi\Delta$  configurations, respectively, in the proton. Eq. 3 readily relates  $a$  and  $b$  to the integral of the asymmetric sea, namely,

$$\int_0^1 [\bar{d}_p(x) - \bar{u}_p(x)]dx = \frac{1}{3}(2a - b), \quad (4)$$

The values for  $a$  and  $b$  from various authors who have employed the meson cloud model show that a typical value of  $b/a$  is  $1/2$ . This leads to  $a = 0.24$ ,  $b = 0.12$  to satisfy the observed flavor asymmetry, resulting in the probability of finding a pion in a nucleon (Eq. 3) of  $a + b = 0.36$ .

While various theoretical models can describe the general trend of the  $\bar{d}/\bar{u}$  asymmetry, they all have difficulties explaining the  $\bar{d}/\bar{u}$  data at large  $x$  ( $x > 0.2$ ). Since the perturbative process gives a symmetric  $\bar{d}/\bar{u}$  while a non-perturbative process is needed to generate an asymmetric  $\bar{d}/\bar{u}$  sea, the relative importance of these two components is directly reflected in the  $\bar{d}/\bar{u}$  ratios. Thus, it would be very important to have new measurements sensitive to the  $\bar{d}/\bar{u}$  ratios at large  $x$  ( $x > 0.2$ ). For given values of  $x_1$  and  $x_2$  the DY cross section is proportional to  $1/s$ , hence the DY cross section at 50 GeV is roughly 16 times greater than that at 800 GeV! The 120 GeV Main Injector at Fermilab and the new 30-50 GeV proton accelerator, J-PARC, present opportunities for extending the  $\bar{d}/\bar{u}$  measurement to larger  $x$  ( $0.25 < x < 0.7$ ). Figure 1 shows the expected statistical accuracy for  $\sigma(p+d)/2\sigma(p+p)$  for an upcoming experiment E906 [12] at Fermilab and a

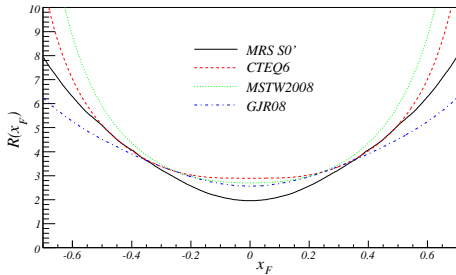


Figure 2: Prediction of the ratio  $(p + p \rightarrow W^+ + x)/(p + p \rightarrow W^- + x)$  at  $\sqrt{s}$  of 500 GeV using various PDFs.

proposed measurement [13] at J-PARC. A definitive measurement of the  $\bar{d}/\bar{u}$  over the region  $0.25 < x < 0.7$  could be obtained.

To disentangle the  $\bar{d}/\bar{u}$  asymmetry from the possible charge-symmetry violation effect [14, 15], one could consider  $W$  boson production in  $p + p$  collision at RHIC. An interesting quantity to be measured is the ratio of the  $p + p \rightarrow W^+ + x$  and  $p + p \rightarrow W^- + x$  cross sections [16]. It can be shown that this ratio is very sensitive to  $\bar{d}/\bar{u}$ . An important feature of the  $W$  production asymmetry in  $p + p$  collision is that it is completely free from the assumption of charge symmetry. Another advantage of  $W$  production in  $p + p$  collision is that it is free from any nuclear effects. Finally, the  $W$  production is sensitive to  $\bar{d}/\bar{u}$  flavor asymmetry at a  $Q^2$  scale of  $\sim 6500 \text{ GeV}^2/c^2$ , significantly larger than all existing measurements. This offers the opportunity to examine the QCD evolution of the sea-quark flavor asymmetry. Figure 2 shows the predictions [17] for  $p + p$  collision at  $\sqrt{s} = 500 \text{ GeV}$ . The MRS S0' corresponds to the  $\bar{d}/\bar{u}$  symmetric parton distributions, while the other three parton distribution functions are from recent global fits with asymmetric  $\bar{d}/\bar{u}$  sea-quark distributions. Figure 2 clearly shows that  $W$  asymmetry measurements at RHIC could provide an independent determination of  $\bar{d}/\bar{u}$ .

### 2.2.2. Unpolarized Drell-Yan angular distribution

The Drell-Yan process [1], in which a charged lepton pair is produced in a high-energy hadron-hadron interaction via the  $q\bar{q} \rightarrow l^+l^-$  process, has been a testing ground for perturbative QCD and a unique tool for probing parton distributions of hadrons. The Drell-Yan production cross sections can be well described by next-to-leading order QCD calculations [18]. This provides a firm theoretical framework for using the Drell-Yan process to

determine the antiquark content of nucleons and nuclei [19], as well as the quark distributions of pions, kaons, and antiprotons [20].

Despite the success of perturbative QCD in describing the Drell-Yan cross sections, it remains a challenge to understand the angular distributions of the Drell-Yan process. Assuming dominance of the single-photon process, a general expression for the Drell-Yan angular distribution is [21]

$$\frac{d\sigma}{d\Omega} \propto 1 + \lambda \cos^2 \theta + \mu \sin 2\theta \cos \phi + \frac{\nu}{2} \sin^2 \theta \cos 2\phi, \quad (5)$$

where  $\theta$  and  $\phi$  denote the polar and azimuthal angle, respectively, of the  $l^+$  in the dilepton rest frame. In the “naive” Drell-Yan model, where the transverse momentum of the quark is ignored and no gluon emission is considered,  $\lambda = 1$  and  $\mu = \nu = 0$  are obtained. QCD effects [22] and non-zero intrinsic transverse momentum of the quarks [23] can both lead to  $\lambda \neq 1$  and  $\mu, \nu \neq 0$ . However,  $\lambda$  and  $\nu$  should still satisfy the relation  $1 - \lambda = 2\nu$  [21]. This so-called Lam-Tung relation, obtained as a consequence of the spin-1/2 nature of the quarks, is analogous to the Callan-Gross relation [24] in Deep-Inelastic Scattering. While QCD effects can significantly modify the Callan-Gross relation, the Lam-Tung relation is predicted to be largely unaffected by QCD corrections [25].

The first measurement of the Drell-Yan angular distribution was performed by the NA10 Collaboration for  $\pi^- + W$  at 140, 194, and 286 GeV/c, with the highest statistics at 194 GeV/c [26]. The  $\cos 2\phi$  angular dependences showed a sizable  $\nu$ , increasing with dimuon transverse momentum ( $p_T$ ) and reaching a value of  $\approx 0.3$  at  $p_T = 2.5$  GeV/c (see Fig. 1). The observed behavior of  $\nu$  could not be described by perturbative QCD calculations which predict much smaller values of  $\nu$  [22]. The Fermilab E615 Collaboration subsequently performed a measurement of  $\pi^- + W$  Drell-Yan production at 252 GeV/c with broad coverage in the decay angle  $\theta$  [27]. The E615 results showed that  $\lambda$  deviates from 1 at large values of  $x_\pi$  (the Bjorken- $x$  of the incident pions), and both  $\mu$  and  $\nu$  have large non-zero values. Furthermore, the E615 data showed that the Lam-Tung relation,  $2\nu = 1 - \lambda$ , is clearly violated.

The NA10 and E615 results on the Drell-Yan angular distributions strongly suggest that new effects beyond conventional perturbative QCD are present. Several attempts have been made to interpret these data. Brandenburg, Nachtmann and Mirke suggested that a factorization-breaking QCD vacuum may lead to a correlation between the transverse spin of the antiquark in

the pion and that of the quark in the nucleon [28]. This would result in a non-zero  $\cos 2\phi$  angular dependence consistent with the data. As pointed out by Boer *et al.*, a possible source for a factorization-breaking QCD vacuum is helicity flip in the instanton model [29]. Several authors have also considered higher-twist effects from quark-antiquark binding in pions [30, 31], motivated by earlier work of Berger and Brodsky [32]. This model predicts behavior of  $\mu$  and  $\nu$  in qualitative agreement with the data. However, the model is strictly applicable only in the  $x_\pi \rightarrow 1$  region while the NA10 and E615 data exhibit nonperturbative effects over a much broader kinematic region.

More recently, Boer pointed out [33] that the  $\cos 2\phi$  angular dependences observed in NA10 and E615 could be due to the  $k_T$ -dependent parton distribution function  $h_1^\perp$ . This so-called Boer-Mulders function [34] is an example of a novel type of  $k_T$ -dependent parton distribution function, and it characterizes the correlation of a quark's transverse spin and its transverse momentum,  $k_T$ , in an unpolarized nucleon. If such correlations are present for both quark and antiquark, they may combine with the transverse spin correlation characteristic of quark-antiquark annihilation in QED to establish a preferred transverse momentum direction producing the  $\cos 2\phi$  dependence. The Boer-Mulders function has an interesting property of being a naive time-reversal odd object and owes its existence to the presence of initial/final state interactions [35]. The Boer-Mulders function is the analog of the Collins fragmentation function [36], which describes the correlation between the transverse spin of a quark and the transverse momentum of the particle into which it hadronizes. Model calculations for the nucleon (pion) Boer-Mulders functions have been carried out [37, 38, 39, 40] in the framework of quark-diquark (quark-spectator-antiquark) model, and can successfully describe the  $\nu$  behavior observed in NA10 [40].

### 3. Drell-Yan and W Production with Polarized Beams and Targets

Measurements of Drell-Yan production with either polarized beams or targets provide access to spin-dependent parton distribution functions (PDF). Polarization, in general, provides access to many additional experimental observables. This section will focus on future DY production experiments performed with polarized proton beams and/or targets, since no experiments have been completed to date, but several are planned [46, 47]. Given that the proton spin is  $\hbar/2$ , the resulting polarization of an ensemble of protons is a (pseudo-) vector quantity. The magnitude of the vector polarization is

the difference in the number of particles with spin parallel to an axis versus the number of particles with spins antiparallel to an axis, scaled by the total number of particles in the ensemble. The direction of the polarization vector is given relative to the incident momentum, and can be either longitudinal or transverse. DY production with longitudinal polarization is sensitive to helicity-difference PDF when either the beam or target are polarized (single-spin), or when both are polarized (two-spin). DY production with transverse polarization is sensitive to transversity PDF for two-spin experiments and to transverse-momentum dependent PDF for single-spin experiments.

The high energies required to ensure sensitivity to partonic degrees of freedom, and hence to DY production, present many significant challenges for the measurement of polarization observables. Among the challenges are technical aspects of producing high-energy polarized beams or preserving target polarization at the high luminosities needed for DY production. Other reviews [48] have described the technical developments that enable these experiments. There are accelerator facilities in operation, or planned, where these experiments will be conducted. At present, polarized proton beams at the high energies needed for polarized DY experiments are available only at the Relativistic Heavy Ion Collider (RHIC) at Brookhaven National Laboratory. Colliding polarized proton beam experiments have been conducted at  $\sqrt{s}=62, 200$  and  $500$  GeV. High-energy polarized beams for fixed target experiments are being considered for the FAIR facility [49], the U70 accelerator at the Institute for High Energy Physics in Protvino and have been proposed for the Main Injector ring at FermiLab.

RHIC is presently the only high-energy accelerator that accelerates and collides spin-polarized protons. Given that it is a collider, the center of mass energy probed is  $62 < \sqrt{s} < 500$  GeV, which is more than an order of magnitude larger collision energy than available to earlier polarized-beam fixed target experiments.

### *3.1. Cross Sections*

The large collision energy leads to the expectation that hadroproduction at RHIC can be described by state-of-the-art pQCD calculations for unpolarized particle production. These calculations are at leading twist, and rely on factorization theorems to evaluate the cross section as a convolution of universal collinear distribution functions, a hard scattering partonic cross section and universal fragmentation functions. Typically, many different partonic scattering diagrams are involved for the production of hadrons.

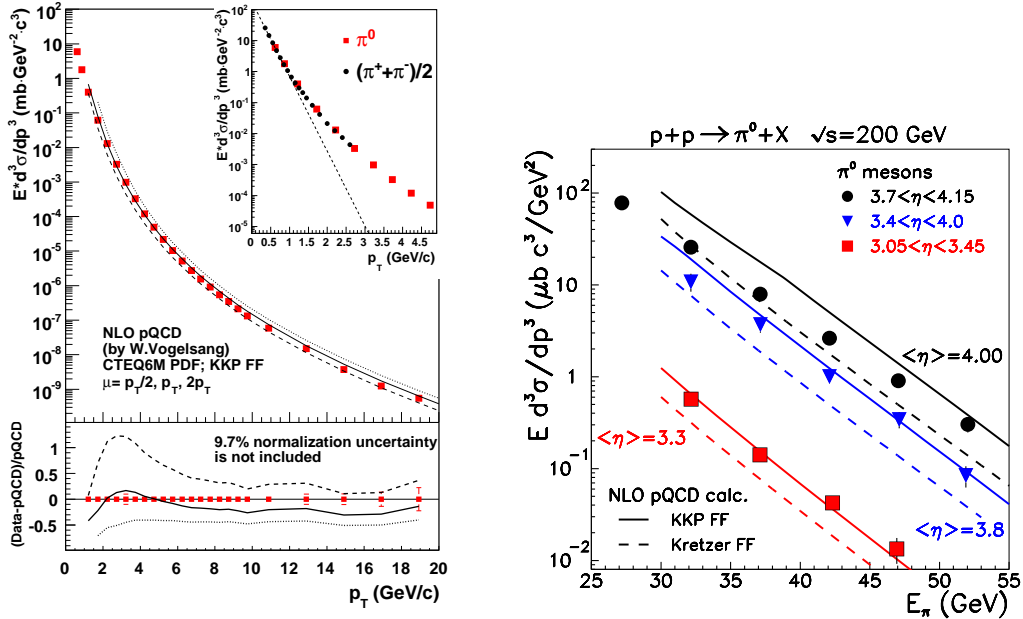


Figure 3: Cross sections for inclusive neutral pion production at  $\sqrt{s}=200$  GeV in comparison to next-to-leading order pQCD calculations. (Left) Results at mid rapidity by the PHENIX collaboration [50, 51] and (Right) Results at large rapidity by the STAR collaboration [58, 53].

In rare processes, like Drell Yan production, there are generally fewer diagrams involved in the calculation. In general, factorization theorems exist for inclusive particle production such as identified hadron production, jet production, direct-photon production and Drell-Yan production. The basic notion of factorization is that a hard scattering process is characterized by the production of a particle, or groups of particles, at large transverse momentum by a partonic interaction, evaluated in a perturbation series in powers of the strong coupling constant. This partonic interaction occurs suddenly and is separated from the non-perturbative structure of the colliding protons or of the hadrons that result from the fragmentation of the scattered partons. The non-perturbative structures are given by the same distribution functions that enter in deep-inelastic scattering and the same fragmentation functions that enter in hadron production at  $e^+e^-$  colliders.

In general, pQCD evaluated at next-to-leading order provides quantitative description of inclusive identified hadron production and jet production

at collision energies probed at RHIC. This description extends down to  $p_T$  of  $\sim 2$  GeV/c and over a broad range of rapidity. Examples for neutral pion production at mid-rapidity and at large rapidity are shown in Fig. 3.

The NLO pQCD calculations in Fig. 3 use distribution functions from a global analysis [54] and fragmentation functions that were available at the time [55, 56]. Subsequently, a global analysis of world data from  $e^+e^-$ , semi-inclusive deep inelastic scattering and cross sections from  $p+p$  collisions [57] have included data from Fig. 3 and shown that it improves the understanding of gluon fragmentation, in particular.

Similar to neutral pion production, measurements from RHIC for charge hadron production [60], inclusive jet production [58] and photon production [59] are found to be in good agreement with NLO pQCD. Analysis of fixed-target, RHIC and Tevatron data for neutral pion and charged hadron production in terms of scaling variables, such as  $x_T = 2p_T/\sqrt{s}$ , have reported contributions to the cross section beyond leading twist [61]. Most recently, RHIC operations at  $\sqrt{s} = 500$  GeV have begun, and first reports of the cross section for the production of  $W^\pm$  bosons have been made [62, 63], and are found to be in good agreement with NLO pQCD.

In general, for less inclusive particle production processes such as di-hadron pairs, di-jet production and photon+jet production, further complexities arise in theoretical descriptions of data. As discussed below, there are good reasons to go beyond inclusive hadron production, to use pairs of hadrons or jets as surrogates for pairs of leptons produced by the Drell Yan process.

The agreement between cross sections and NLO pQCD calculations are the foundation then for understanding spin observables measured by the collision of spin-polarized beams at RHIC. The spin observables receiving greatest attention at RHIC are defined in Sec. 3.2.

### 3.2. Spin Observables

A primary objective of spin physics at RHIC is to measure quantities that are sensitive to possible gluon polarization contributions to the spin of the proton. Such measurements address a question about the spin sum rule for the proton. Measurements have been completed for the double longitudinal spin correlation

$$A_{LL} = \frac{\sigma_{++} - \sigma_{+-}}{\sigma_{++} + \sigma_{+-}} \quad (6)$$

for mid-rapidity  $\pi^0$  at  $\sqrt{s}=62$  and 200 GeV and for midrapidity jet production at  $\sqrt{s}=200$  GeV. These probes have a quadratic dependence on  $\Delta g$  given the admixture of  $gg$ ,  $qg$  and  $qq'$  partonic scatterings that lead to the particle production. The average gluon momentum fraction is given by  $x_T = 2p_T/\sqrt{s}$ , so the data probes for gluon polarization from  $\sim 0.01 < x_T < 0.2$ . In Eqn. 6,  $\sigma_{++}$  refers to the cross section when the colliding protons have the same helicity and  $\sigma_{+-}$  refers to the cross section when the colliding protons have opposite helicity. These helicity-dependent cross sections are accessed by experimentally measuring spin-dependent particle production yields ( $N_{++}$  and  $N_{+-}$ ), and then scaling these yields by measurements of spin-dependent luminosities ( $\mathcal{L}_{++}$  and  $\mathcal{L}_{+-}$ ) and by measurements of the polarizations of each beam ( $P_{b1}$  and  $P_{b2}$ ). In terms of measured quantities,

$$A_{LL} = \frac{1}{P_{b1}P_{b2}} \frac{N_{++}/\mathcal{L}_{++} - N_{+-}/\mathcal{L}_{+-}}{N_{++}/\mathcal{L}_{++} + N_{+-}/\mathcal{L}_{+-}} = \frac{1}{P_{b1}P_{b2}} \frac{N_{++} - \mathcal{R}N_{+-}}{N_{++} + \mathcal{R}N_{+-}}, \quad (7)$$

where  $\mathcal{R} = \mathcal{L}_{++}/\mathcal{L}_{+-}$  is the spin-dependent relative luminosity. The beam polarizations entering Eqn. 7 have their magnitude measured by  $p^\uparrow p^\uparrow$  elastic scattering from a polarized internal target [64], and their directions measured by so-called local polarimeters that are sensitive to transverse polarization components from particle production that has a non-zero analyzing power (as defined in Eqn. 8).

Even though the the primary focus was initially on measuring  $A_{LL}$ , the experiments at RHIC have also measured transverse single spin asymmetries

$$A_N = \frac{\sigma^\uparrow - \sigma^\downarrow}{\sigma^\uparrow + \sigma^\downarrow}, \quad (8)$$

where  $\sigma^\uparrow$  refers to the cross section for collisions involving spin-up transversely polarized protons and  $\sigma^\downarrow$  refers to the cross section for spin-down transversely polarized protons. These spin effects were crucial for identifying local polarimeters, and proved interesting in their own right as discussed in Sec. 3.3.1.

As discussed in detail in Sec. 3.3, transverse single spin asymmetries are parity conserving and depend on  $\mathbf{S} \cdot (\mathbf{p}_1 \times \mathbf{p}_2)$ , where  $S$  is the proton spin direction transverse to a plane defined by two momentum vectors  $p_{1(2)}$ . Given this form, the measured yield for particle production with a non-zero  $A_N$  acquires an azimuthal modulation,  $\cos\phi$ , where  $P_{beam} \cos\phi$  gives the component of the beam polarization perpendicular to the reaction plane. Consequently,

there are multiple ways to measure  $A_N$ :

$$A_N = \frac{1}{P_{beam}} \frac{N^\uparrow/\mathcal{L}^\uparrow - N^\downarrow/\mathcal{L}^\downarrow}{N^\uparrow/\mathcal{L}^\uparrow + N^\downarrow/\mathcal{L}^\downarrow}, \quad (9)$$

$$A_N = \frac{1}{P_{beam}} \frac{N_L/\Delta\Omega_L - N_R/\Delta\Omega_R}{N_L/\Delta\Omega_L + N_R/\Delta\Omega_R}, \quad (10)$$

$$A_N \approx \frac{1}{P_{beam}} \frac{\sqrt{N_L^\uparrow N_R^\downarrow} - \sqrt{N_L^\downarrow N_R^\uparrow}}{\sqrt{N_L^\uparrow N_R^\downarrow} + \sqrt{N_L^\downarrow N_R^\uparrow}}. \quad (11)$$

Eqn. 9 refers to use of a single detector at fixed polar and azimuthal angles. The measurement is performed by measuring the yield for spin-up and spin-down beam polarizations, and by measuring the luminosities ( $\mathcal{L}^{\uparrow,\downarrow}$ ) for these two possibilities. Eqn. 10 refers to use of mirror symmetric detector pairs, with one detector of effective solid angle  $\Delta\Omega_L$  positioned at  $\phi = 0$  and a second detector of effective solid angle  $\Delta\Omega_R$  positioned at  $\phi = \pi$ . The effective solid angle is given by the product of the geometric acceptance and efficiency of the detectors. Eqn. 11 is the so-called cross-ratio measurement that eliminates the requirements of concurrent measurements of spin-dependent luminosity ( $\mathcal{L}^{\uparrow,\downarrow}$  and detector solid angles ( $\Delta\Omega_{L,R}$ ) by exploiting a mirror symmetric pair of detectors and reversing the beam polarizations.

Such measurements were required to identify local polarimeters for the RHIC experiments, for robust measurements of  $A_{LL}$  because the stable spin direction of the beams in RHIC are vertical. Longitudinal polarization is produced at the interaction points by helical-dipole spin rotator magnets. These magnets precess the polarization into the bend-plane of the ring. The spins further precess through the insertion magnets to produce longitudinal polarization for the colliding beams. The resulting polarization direction for collisions is a sensitive function of the currents through the spin-rotator magnets, so local polarimeters sensitive to remnant polarization components are a requirement. At least two such different particle productions have been found to have large enough  $A_N$  and sufficient event rate to serve as local polarimeters. A common local polarimeter at RHIC is neutron production in the far forward direction [65] and the spin-dependent topological distribution of forward particle production.

Longitudinal single-spin asymmetries are parity violating, so are expected to be zero in strong interaction particle production and large in weak interaction particle production. These asymmetries are a focus at RHIC, because of

their sensitivity to flavor dependence of quark and antiquark polarizations, as discussed in Sec. 3.4. They are defined as

$$A_L = \frac{\sigma_+ - \sigma_-}{\sigma_+ + \sigma_-}, \quad (12)$$

and require measurement of particle production with one longitudinally polarized beam colliding with an unpolarized beam. The parity-violating asymmetry is the difference of the positive and negative helicity cross sections divided by their sum. Analogous to  $A_{LL}$ , this parity violating asymmetry consists of measuring single-beam helicity dependent yields ( $N_{+/-}$ ), spin-dependent luminosities ( $\mathcal{L}_{+/-}$ ) and measurement of the beam polarization, so that Eqn. 12 becomes in terms of measured quantities:

$$A_L = \frac{1}{P_{beam}} \frac{N_+/\mathcal{L}_+ - N_-/\mathcal{L}_-}{N_+/\mathcal{L}_+ + N_-/\mathcal{L}_-}. \quad (13)$$

As for  $A_{LL}$ , local polarimeters are required to minimize transverse polarization components by tuning spin rotator magnets near the STAR and PHENIX interaction regions.

We now discuss special cases of these spin observables, in the context of what has been learned so far at RHIC and in the outlook for their measurement for Drell Yan production.

### 3.3. Transverse Single Spin Asymmetries

Transverse single spin asymmetries (SSA) are a general class of experimental observable having the form  $\mathbf{S} \cdot (\mathbf{p}_1 \times \mathbf{p}_2)$ , where  $\mathbf{S}$  is the spin vector, perpendicular to a plane defined by two momenta ( $\mathbf{p}_1, \mathbf{p}_2$ ). Transverse SSA conserve parity, but are expected to be small in leading-twist, collinear pQCD due to the chiral nature of the theory [66], especially when only light quarks are considered. As described in more detail below, transverse SSA are found to be large by experiments. This has prompted extensions to theory to include spin-correlated transverse momentum dependence (TMD) in distribution [67] and fragmentation functions [68]. There are factorization theorems that facilitate use of TMD distribution functions for DY production [69]. There are not factorization theorems for the use of TMD distribution or fragmentation functions to describe the production of hadrons or photons. Generalized parton models [70] that include transverse momentum dependence have been used to gain insights by comparison to measurement.

The lack of TMD factorization theorems for all but DY has prompted development twist-3 calculations to explain data in terms of  $qg$  and  $gg$  correlations. It has been shown that moments of specific TMD distribution functions can be related the partonic correlators that enter for twist-3 calculations.

Given that this review is primarily on DY production, more emphasis is given to the TMD extensions to leading-twist, collinear pQCD, although to understand the intense interest in polarized DY production, it is first necessary to review single-spin asymmetries for hadro-production, and to mention results from semi-inclusive deep inelastic scattering.

### 3.3.1. Observables in Hadroproduction

Initially motivated by the search for local polarimeters,  $A_N$  has been measured for inclusive pion production by the STAR collaboration [72, 53] at  $\sqrt{s} = 200$  GeV (Fig. 4). Neutral pions play a special role for such measurements since simple electromagnetic calorimeters with sufficient granularity can identify  $\pi^0$  production from its two photon decay, even for very high energy pions. The STAR measurements employed mirror-symmetric electromagnetic calorimeters that viewed forward particle production through large holes in the poletips of the solenoidal magnet. Given the mirror-symmetry,  $A_N$  was measured using Eqn. 11, thus minimizing systematic errors. As observed at lower collision energy,  $A_N$  increases as the Feynman- $x$  of the neutral pion increases ( $x_F = 2p_L/\sqrt{s}$ , scaling the longitudinal momentum of the produced particle by its maximum possible value). This same  $x_F$  dependence has been observed at for pion production by FermiLab E704 [71] and in polarized proton collisions at even lower  $\sqrt{s}$ . Unlike the situation at lower  $\sqrt{s}$ , the cross sections at RHIC energies are in good agreement with NLO pQCD (Fig. 3) in the same rapidity range where  $A_N$  is measured to be large.

The BRAHMS experiment at RHIC [73] consisted of a forward spectrometer (FS) and a midrapidity magnetic spectrometer. The FS was capable of identifying pions and kaons up to  $p \sim 35$  GeV/c using a Ring Imaging Cherenkov Detector [74]. The pseudorapidity coverage and particle identification capabilities were well matched to measure  $A_N$  to high  $x_F$  for polarized proton collisions at  $\sqrt{s}=62$  GeV [75]. The BRAHMS measurement of  $A_N$  relied on Eqn. 9 and required a concurrent measurement of spin-dependent luminosity. Their results are shown in Fig. 5. The data shows positive  $A_N$  for  $\pi^+$  production and negative  $A_N$  for  $\pi^-$  production, and the magnitude of  $A_N$  increasing with  $x_F$ , as was observed by E704 [71] at lower  $\sqrt{s}$ .

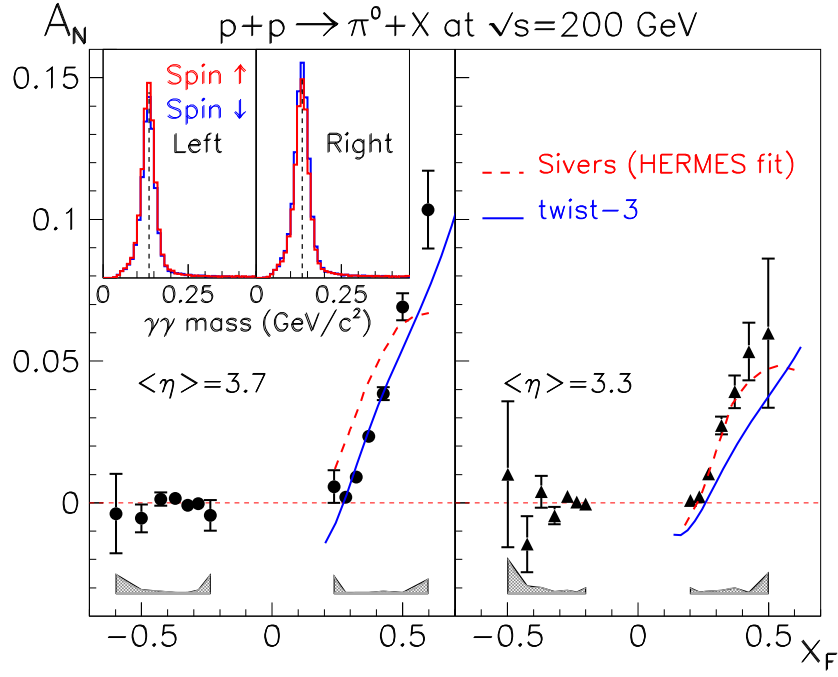


Figure 4: The analyzing power for the production of neutral pions in  $\sqrt{s} = 200$  GeV polarized proton collisions.  $A_N$  is measured as a function of  $x_F = 2p_L/\sqrt{s}$  by the STAR collaboration [72]. The measurements are reported at two different pseudorapidity values. The calculations are described in the text. The inset shows examples of the spin-sorted invariant mass distributions from mirror symmetric detectors. The vertical lines mark the  $\pi^0$  mass.

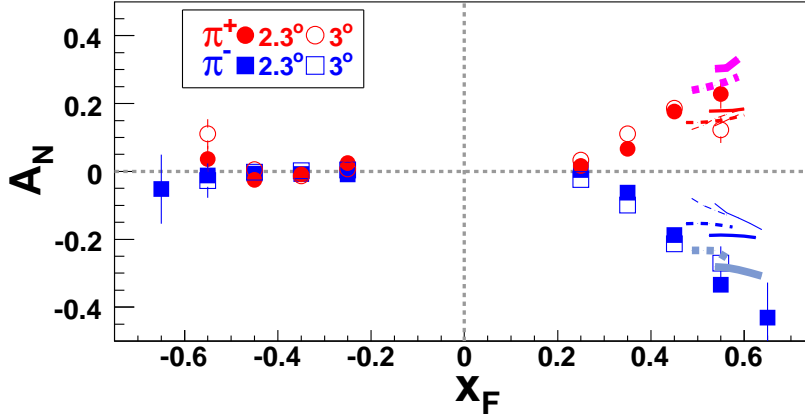


Figure 5: Analyzing power for identified charged pions measured as a function of  $x_F$  in  $\sqrt{s} = 62$  GeV polarized proton collisions by the BRAHMS collaboration [75]. The measurements are reported at two different pseudorapidity values. The calculations are described in the text.

These measurements at RHIC were essentially concurrent with measurements of semi-inclusive deep inelastic scattering (SIDIS) from transversely polarized proton targets [76, 77]. These results have been recently reviewed [78]. A key distinction between the SIDIS results on transverse SSA and the RHIC results on  $A_N$  is that for the former, there are two scales set by the virtuality of the photon ( $Q^2$ ) exchanged when scattering the lepton and by the transverse momentum of the measured hadron. The RHIC results for transverse single spin asymmetry are for inclusive particle production, so have a single scale, set by the transverse momentum of the produced particle.

Theoretical pictures of what gives rise to these spin effects had been developed soon after the E704 measurements were reported [71], and require extensions to the leading-twist collinear pQCD description of particle production. In the Sivers effect [67], a spin-correlated transverse momentum ( $k_T$ ) is attributed to the quark within the proton, in addition to the longitudinal momentum fraction  $x$ . In the Collins effect [68], a transversely polarized quark is found within a transversely polarized proton. Following a scattering, this transversely polarized quark reveals its spin direction through spin-correlated and transverse momentum dependent fragmentation. Both of these effects involve transverse momentum dependence (TMD) in either distribution or fragmentation functions. Spin-correlated transverse momentum dependence in a distribution function describes orbital motion, which

is currently of great interest in attempts to identify how the constituents of the proton give rise to its intrinsic spin. Factorization theorems that use TMD distribution functions have only been proven for DY production. For the case of pion production in polarized  $p + p$  collisions, a collinear twist-3 factorization has been developed [79] for which  $qg$  correlations [80] play a central role. Recent work has related moments of the Sivers function to the  $qg$  correlators [81] that appear in the collinear twist-3 approach, indicating an intimate relationship between these approaches. The complexities that arise in using TMD distribution functions for pion production in polarized proton collisions are vastly simplified for Drell Yan production. We proceed to describe TMD.

### 3.3.2. *Transverse Momentum Dependent Parton Distribution Functions*

Ordinary parton distribution functions (PDF) depend on the fraction  $x$  of the proton momentum carried by a quark, antiquark or gluon, collectively referred to as a parton. These distributions depend on the scale at which they are observed. For deep inelastic scattering, this scale is given by the squared space-like virtuality  $Q^2$  of the exchanged photon. For Drell-Yan production, the photon virtuality is time-like and the scaling is determined by the mass  $M$  of the virtual photon produced in the  $q\bar{q}$  annihilation. Rigorous factorization theorems have been proven where universal PDF enter convolution integrals to predict inclusive cross sections for many hard scattering processes. The resolution scale for the PDF are typically set by the transverse momentum,  $p_T$ , for the particle production in general hard scattering processes. Scale dependence is predicted by pQCD evolution equations, once PDF are established at one resolution scale by experiment. Scale-dependent evolution redistributes the longitudinal momenta of the partons within the proton.

A second resolution scale enters for particle production processes that are less inclusive. For example, semi-inclusive deep inelastic scattering (SIDIS) involves detection of one or more hadrons in coincidence with the scattered lepton. In this case, there is a transverse momentum of the hadron relative to the virtual photon. Dileptons ( $e^+e^-$  or  $\mu^+\mu^-$  pairs) are experimentally observed in Drell Yan production. The dilepton has a mass and has longitudinal and transverse momentum components. The hadron transverse momentum in SIDIS and the virtual photon transverse momentum in DY set a second resolution scale given by its transverse momentum.

Transverse-momentum dependent PDF are one generalization of ordinary

PDF to account for processes like SIDIS and the  $p_T$  dependence of DY production when the transverse momentum is small compared to the virtuality of the photon. Factorization theorems have been proven for TMD PDF for SIDIS and DY production. Unlike for ordinary PDF, complications enter for TMD for more general hard scattering processes.

There is broad utility for the experimental and theoretical investigations of ordinary PDF. On the one hand, PDF are essential in the search for new particles, in that they enter theoretical calculations that predict how such particles are produced in  $pp$  or  $ep$  collisions. As well, the backgrounds for ordinary particle production must be well understood for new particle searches. On the other hand, the PDF provide our understanding of the structure of hadrons, and in particular the proton. The generalization of the PDF to include transverse momentum dependence provides an intrinsically richer picture of the internal structure of the proton.

TMD that depend on spin are particularly interesting. The first polarized Drell Yan experiments have primary focus on the Sivers function, generally referred to in the literature as  $f_{1T}^\perp(x, k_\perp)$ , where  $k_\perp$  is the transverse momentum of the parton within a transversely polarized proton. The general form of the polarized DY cross section has a rich structure with sensitivity to many spin-dependent PDF, in both the collinear and TMD case. The Sivers function results in spin effects of the form  $\vec{S}_p \cdot \vec{p} \times \vec{k}_\perp$ , where  $\vec{S}_p$  refers to the proton spin and  $\vec{p}$  refers to the proton momentum. The particular interest in the Sivers function for the first polarized DY experiments is because it was expected to be zero due to naive time reversal [36]. Naive time reversal invariance is broken by the presence of initial-state or final-state interactions. For semi-inclusive deep inelastic scattering, final-state interactions allow [35] for a non-zero  $f_{1T}^\perp$ . For Drell Yan production, initial-state interactions allow for a non-zero  $f_{1T}^\perp$ . The nature of these interactions leads to the robust theoretical prediction [84]

$$f_{1T}^\perp|^{DIS} = -f_{1T}^\perp|^{DY}. \quad (14)$$

This theoretical prediction will soon be tested by experiment.

### 3.3.3. Outlook for Polarized Drell Yan Production

We anticipate that the first experiments that measure transverse SSA for DY production will be completed in the next few years. There are two such experiments that are most likely to be conducted first.

The COMPASS collaboration at CERN proposes to use a  $\pi^-$  beam of momentum  $p=190$  GeV/c incident on a transversely polarized  $\text{NH}_3$  target and detect  $\mu^+\mu^-$  pairs with their apparatus that has been extensively used for deep inelastic scattering studies. The secondary  $\pi^-$  flux of  $6 \times 10^7$  particles/s will provide COMPASS with a luminosity of  $1.7 \times 10^{33}$   $\text{cm}^{-2}\text{s}^{-1}$ . Background reduction requires the addition of an absorber placed downstream of the polarized target. Tests with an absorber have been conducted, and dimuons were observed. In a 2-year run, they project statistical uncertainties of  $\delta A_N \sim 0.014$  for dimuons of mass  $4 < M_{\mu\mu} < 9$  GeV/c<sup>2</sup>.

At RHIC, the focus is on detecting forward dileptons, given the pattern of transverse SSA in pion production, strongly favoring these spin effects for large  $x_F$ . STAR and PHENIX are considering major forward instrumentation upgrades, in part motivated by DY production studies. Calorimetry plays a central role, and can be used for identifying  $e^+e^-$  pairs produced by the Drell Yan mechanism. Prolific hadronic backgrounds are suppressed by characterizing the longitudinal and transverse shower profiles in an electromagnetic calorimeter. Photons are suppressed by preshower detectors with sufficient granularity to handle multi-particle final states. ...

The preferred collision energy for polarized proton collisions to produce dileptons by Drell Yan production is  $\sqrt{s}=500$  GeV. The large collision energy is where the collision luminosity is greatest. As well, the partonic luminosity grows because  $x_2$  (antiquark momentum fraction) decreases rapidly with increasing  $\sqrt{s}$ . ...

### *3.4. Longitudinal single-spin observables*

## **4. Intrinsic Quark Components of the Nucleons and Hadron Production**

### *4.1. Intrinsic Heavy-Quark Sea of the Nucleons*

The origin of sea quarks of the nucleons remains a subject of intense interest in hadron physics. Brodsky, Hoyer, Peterson, and Sakai (BHPS) [41] suggested some time ago that there are two distinct components of the nucleon sea. The first is called the “extrinsic” sea originating from the splitting of gluons into  $Q\bar{Q}$  pairs. This extrinsic sea can be well described by quantum chromodynamics (QCD). Another component of the nucleon sea is the “intrinsic” sea which has a nonperturbative origin. In particular, the  $|uudQ\bar{Q}\rangle$  five-quark Fock states can lead to the “valence-like” intrinsic sea for the  $Q$

and  $\bar{Q}$  in the proton. This intrinsic component is expected to carry a relatively large momentum fraction  $x$ , in contrast to the extrinsic one peaking at the small- $x$  region. The presence of the intrinsic charm component can lead to a sizable charm production at the forward rapidity ( $x_F$ ) region.

The  $x$  distribution of the intrinsic charm in the BHPS model was derived with some simplifying assumptions. Recently, Pumplin [42] showed that a variety of light-cone models in which these assumptions are removed would still predict the  $x$  distributions of the intrinsic charm similar to that of the BHPS model. The CTEQ collaboration [42] has also examined all relevant hard-scattering data sensitive to the presence of the IC component, and concluded that the existing data are consistent with a wide range of the IC magnitude, from null to 2-3 times larger than the estimate by the BHPS model. This result shows that the experimental data are not yet sufficiently accurate to determine the magnitude or the  $x$  distribution of the IC.

#### 4.2. Intrinsic Light-Quark Sea of the Nucleons

The BHPS model predicts the probability for the  $uudQ\bar{Q}$  five-quark Fock state to be approximately proportional to  $1/m_Q^2$ , where  $m_Q$  is the mass of the quark  $Q$  [41]. Therefore, the light five-quark states  $uudu\bar{u}$  and  $uudd\bar{d}$  are expected to have significantly larger probabilities than the  $uudc\bar{c}$  state. This suggests that the light quark sector could potentially provide more clear evidence for the roles of the five-quark Fock states, allowing the specific predictions of the BHPS model, such as the shape of the quark  $x$  distributions originating from the five-quark configuration, to be tested.

To compare the experimental data with the prediction based on the intrinsic five-quark Fock state, it is essential to separate the contributions of the intrinsic quark and the extrinsic one. Fortunately, there exist some experimental observables which are free from the contributions of the extrinsic quarks. As discussed later, the  $\bar{d} - \bar{u}$  and the  $\bar{u} + \bar{d} - s - \bar{s}$  are examples of quantities independent of the contributions from extrinsic quarks. The  $x$  distribution of  $\bar{d} - \bar{u}$  has been measured in a Drell-Yan experiment [43]. A recent measurement of  $s + \bar{s}$  in a semi-inclusive deep-inelastic scattering (DIS) experiment [44] also allowed the determination of the  $x$  distribution of  $\bar{u} + \bar{d} - s - \bar{s}$ .

For a  $|uudQ\bar{Q}\rangle$  proton Fock state, the probability for quark  $i$  to carry a

momentum fraction  $x_i$  is given in the BHPS model [41] as

$$P(x_1, \dots, x_5) = N_5 \delta(1 - \sum_{i=1}^5 x_i) [m_p^2 - \sum_{i=1}^5 \frac{m_i^2}{x_i}]^{-2}, \quad (15)$$

where the delta function ensures momentum conservation.  $N_5$  is the normalization factor for five-quark Fock state, and  $m_i$  is the mass of quark  $i$ . In the limit of  $m_{4,5} \gg m_p, m_{1,2,3}$ , where  $m_p$  is the proton mass, Eq. 15 becomes

$$P(x_1, \dots, x_5) = \tilde{N}_5 \frac{x_4^2 x_5^2}{(x_4 + x_5)^2} \delta(1 - \sum_{i=1}^5 x_i), \quad (16)$$

where  $\tilde{N}_5 = N_5/m_{4,5}^4$ . Eq. 16 can be readily integrated over  $x_1, x_2, x_3$  and  $x_4$ , and the heavy-quark  $x$  distribution [41, 42] is:

$$P(x_5) = \frac{1}{2} \tilde{N}_5 x_5^2 \left[ \frac{1}{3} (1 - x_5)(1 + 10x_5 + x_5^2) - 2x_5(1 + x_5) \ln(1/x_5) \right]. \quad (17)$$

One can integrate Eq. 17 over  $x_5$  and obtain the result  $\mathcal{P}_5^{c\bar{c}} = \tilde{N}_5/3600$ , where  $\mathcal{P}_5^{c\bar{c}}$  is the probability for the  $|uudc\bar{c}\rangle$  five-quark Fock state. An estimate of the magnitude of  $\mathcal{P}_5^{c\bar{c}}$  was given by Brodsky et al. [41] as  $\approx 0.01$ , based on diffractive production of  $\Lambda_c$ . This value is consistent with a bag-model estimate [45].

#### 4.3. Prospect of Future Hadron Production Experiments for Probing Heavy-Quark Sea

### References

- [1] S.D. Drell and T.M. Yan, Phys. Rev. Lett. **25**, 316 (1970); Ann. Phys. (NY) **66**, 578 (1971).
- [2] J.M. Conrad, M.H. Shaevitz and T. Bolton, Rev. Mod. Phys. **70** (1998) 1341.
- [3] K. Gottfried, Phys. Rev. Lett. **18** (1967) 1174.
- [4] P. Amaudruz *et al.*, Phys. Rev. Lett. **66** (1991) 2712.
- [43] E.H. Hawker *et al.*, Phys. Rev. Lett. **80** (1998) 3715.

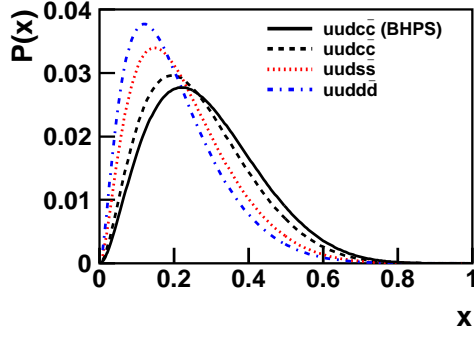


Figure 6: The  $x$  distributions of the intrinsic  $\bar{Q}$  in the  $uudQ\bar{Q}$  configuration of the proton from the BHPS model [41]. The solid curve is plotted using the expression in Eq. 17 for  $\bar{c}$ . The other three curves, corresponding to  $\bar{c}$ ,  $\bar{s}$ , and  $\bar{d}$  in the five-quark configurations, are obtained by solving Eq. 15 numerically. The same probability  $\mathcal{P}_5^{Q\bar{Q}}$  ( $\mathcal{P}_5^{Q\bar{Q}} = 0.01$ ) is used for the three different five-quark states.

- [6] J.C. Peng *et al.*, Phys. Rev. **D58** (1998) 092004.
- [7] R.S. Towell *et al.*, Phys. Rev. **D64** (2001) 052002.
- [8] S. Kumano, Phys. Rep. **303** (1998) 183.
- [9] G.T. Garvey and J.C. Peng, Prog. Part. Nucl. Phys. **47** (2001) 203.
- [10] A. W. Thomas, Phys. Lett. **B126** (1983) 97.
- [11] J. D. Sullivan, Phys. Rev. **D5** (1972) 1732.
- [12] E906 Collaboration, D.F. Geesaman *et al.*, Fermi National Accelerator Laboratory Proposal E906, 1999.
- [13] J.C. Peng, S. Sawada *et al.*, hep-ph/0007341.
- [14] B.Q. Ma, Phys. Lett. **B274** (1992) 111.
- [15] C. Boros, J.T. Londergan and A.W. Thomas, Phys. Rev. Lett. **81** (1998) 4075.
- [16] J.C. Peng and D.M. Jansen, Phys. Lett. **B354** (1995) 460.
- [17] R. Yang, J.C. Peng and M. Grosse-Perdekamp, Phys. Lett. **B680** (2009) 231.

- [18] W.J. Stirling and M.R. Whalley, *J. Phys.* **G19**, D1 (1993).
- [19] P.L. McGaughey, J.M. Moss, and J.C. Peng, *Annu. Rev. Nucl. Part. Sci.* **49**, 217 (1999).
- [20] I.R. Kenyon, *Rep. Prog. Phys.* **45**, 1261 (1982); K. Freudenreich, *Int. J. Mod. Phys.* **A5**, 3643 (1990).
- [21] C.S. Lam and W.K. Tung, *Phys. Rev.* **D18**, 2447 (1978).
- [22] P. Chiappetta and M. LeBellac, *Z. Phys.* **C32**, 521 (1986).
- [23] J. Cleymans and M. Kuroda, *Phys. Lett.* **B105**, 68 (1981).
- [24] C.G. Callan and D. J. Gross, *Phys. Rev. Lett.* **22**, 156 (1969).
- [25] C.S. Lam and W.K. Tung, *Phys. Rev.* **D21**, 2712 (1980).
- [26] NA10 Collaboration, S. Falciano *et al.*, *Z. Phys.* **C31**, 513 (1986); M. Guanziroli *et al.*, *Z. Phys.* **C37**, 545 (1988).
- [27] E615 Collaboration, J.S. Conway *et al.*, *Phys. Rev.* **D39**, 92 (1989); J.G. Heinrich *et al.*, *Phys. Rev.* **D44**, 1909 (1991).
- [28] A. Brandenburg, O. Nachtmann, and E. Mirkes, *Z. Phys.* **C60**, 697 (1993).
- [29] D. Boer, A. Brandenburg, O. Nachtmann, and A. Utermann, *Eur. Phys. J.* **C40**, 55 (2005).
- [30] A. Brandenburg, S.J. Brodsky, V.V. Khoze, and D. Müller, *Phys. Rev. Lett.* **73**, 939 (1994).
- [31] K.J. Eskola, P. Hoyer, M. Vântinnen, and R. Vogt, *Phys. Lett.* **B333**, 526 (1994).
- [32] E.L. Berger and S.J. Brodsky, *Phys. Rev. Lett.* **42**, 940 (1979).
- [33] D. Boer, *Phys. Rev.* **D60**, 014012 (1999).
- [34] D. Boer and P.J. Mulders, *Phys. Rev.* **D57**, 5780 (1998).
- [35] S.J. Brodsky, D.S. Hwang, and I. Schmidt, *Phys. Lett.* **B530**, 99 (2002).

- [36] J.C. Collins, Nucl. Phys. **B396**, 161 (1993).
- [37] L.P. Gamberg, G.R. Goldstein, and K.A. Oganessyan, Phys. Rev. **D67**, 071504(R) (2003).
- [38] D. Boer, S.J. Brodsky, and D.S. Hwang, Phys. Rev. **D67**, 054003 (2003).
- [39] A. Bacchetta, A. Schäfer, and J.-J. Yang, Phys. Lett. **B578**, 109 (2004).
- [40] Z. Lu and B.-Q. Ma, Phys. Lett. **B615**, 200 (2005).
- [41] S.J. Brodsky, P. Hoyer, C. Peterson, and N. Sakai, Phys. Lett. B **93**, 451 (1980); S.J. Brodsky, C. Peterson, and N. Sakai, Phys. Rev. D **23**, 2745 (1981).
- [42] J. Pumplin, Phys. Rev. D **73**, 114015 (2006); J. Pumplin, H. L. Lai, and W. K. Tung, Phys. Rev. D **75**, 054029 (2007).
- [43] E. A. Hawker *et al.* (E866/NuSea Collaboration), Phys. Rev. Lett. **80**, 3715 (1998); J. C. Peng *et al.*, Phys. Rev. D **58**, 092004 (1998); R.S. Towell *et al.*, Phys. Rev. D **64**, 052002 (2001).
- [44] A. Airapetian *et al.* (HERMES Collaboration), Phys. Lett. B **666**, 446 (2008).
- [45] J. F. Donoghue and E. Golowich, Phys. Rev. D **15**, 3421 (1977).
- [46] COMPASS collaboration, COMPASS II proposal, CERN-SPSC-2010-014, SPSC-P-340 (2010) [<http://cdsweb.cern.ch/record/1265628/files/SPSC-P-340.pdf>].
- [47] E. C. Aschenauer *et al.*, *Large Rapidity Drell Yan Production at RHIC*, proposal to Brookhaven National Laboratory program committee (2011) [[http://www.bnl.gov/npp/docs/pac0611/DY\\_pro\\_110516\\_final.2.pdf](http://www.bnl.gov/npp/docs/pac0611/DY_pro_110516_final.2.pdf)].
- [48] G. Bunce, N. Saito, J. Soffer, W. Vogelsang, Annu. Rev. Nucl. Part. Sci. **50**, 525 (2000).
- [49] A. Lehrach *et al.*, Int. J. Mod. Phys. E **18**, 420 (2009).
- [50] A. Adare *et al.* (PHENIX), Phys. Rev. D **76**, 051106 (2007).
- [51] S. S. Adler *et al.* (PHENIX), Phys. Rev. Lett. **91**, 241803 (2003).

- [58] J. Adams *et al.* (STAR), Phys. Rev. Lett. **97**, 152302 (2006).
- [53] J. Adams *et al.* (STAR), Phys. Rev. Lett. **92**, 171801 (2004).
- [54] J. Pumplin *et al.*, J. High Energy Phys. **07**, 012 (2002).
- [55] B. A. Kniehl *et al.*, Nucl. Phys. B**597**, 337 (2001).
- [56] S. Kretzer, Phys. Rev. D **62**, 054001 (2000).
- [57] D. de Florian, R. Sassot, M. Stratmann, Phys. Rev. D **75**, 114010 (2007).
- [58] B. I. Abelev *et al.* (STAR), Phys. Rev. Lett. **97**, 252001 (2006).
- [59] S. S. Adler *et al.* (PHENIX), Phys. Rev. Lett. **98**, 012002 (2007).
- [60] I. Arsene *et al.* (BRAHMS), Phys. Rev. Lett. **98**, 252001 (2007).
- [61] F. Arleo, S. J. Brodsky, D. S. Hwang, A. M. Sickles, Proceedings of the 45<sup>th</sup> Rencontres de Moriond on QC and High Energy Interactions, La Thuile (2010) [arXiv:1006.4045].
- [62] A. Adare *et al.* (PHENIX), Phys. Rev. Lett. **106**, 062001 (2011).
- [63] G. Agakishiev *et al.* (STAR), submitted to Phys. Rev. D [arXiv:1112.2980].
- [64] H. Okada *et al.*, Phys. Lett. B **638**, 450 (2006).
- [65] Y. Fukao *et al.*, Phys. Lett. B **650**, 325 (2007).
- [66] G. L. Kane, J. Pumplin, W. Repko, Phys. Rev. Lett. **41**, 1689 (1978).
- [67] D. Sivers, Phys. Rev. D **41**, 83 (1990); **43**, 261 (1991).
- [68] J. Collins, Nucl. Phys. B **396**, 161 (1993)
- [69] J. C. Collins, D. E. Soper, G. Sterman, Nucl. Phys. B **261**, 104 (1985); **308**, 833 (1988).
- [70] U. D'Alesio, F. Murgia, Prog. Part. Nucl. Phys. **61**, 394 (2008).
- [71] B. E. Bonner *et al.* Phys. Rev. Lett. **61**, 1918 (1988); A. Bravar *et al.*, *ibid.* **77**, 2626 (1996); D. L. Adams *et al.*, Phys. Lett. B **261**, 201 (1991); **264**, 462 (1991; Z. Phys. C **56**, 181 (1992).

- [72] B. I. Abelev *et al* (STAR), Phys. Rev. Lett. **101**, 222001 (2008).
- [73] M. Adamczyk *et al.* (BRAHMS), Nucl. Inst. Meth. A **499**, 437 (2003).
- [74] R. Debbe *et al.*, Nucl. Inst. Meth. A **570**, 216 (2007).
- [75] I. Arsene *et al* (BRAHMS), Phys. Rev. Lett. **101**, 042001 (2008).
- [76] A. Airapetian *et al.* (HERMES), Phys. Rev. Lett. **103**, 152002 (2009).
- [77] F. Bradamante (for COMPASS), invited talk at *3<sup>rd</sup> International Workshop on Transverse Polarization Phenomena in Hard Scattering* (2011) [arXiv:1111.0869].
- [78] M. Burkardt, A. Miller and W. D. Nowak, Rept. Prog. Phys. **73**, 016201 (2010).
- [79] J. Qiu and G. Sterman, Phys. Rev. D**59**, 014004 (1998).
- [80] A. V. Efremov and O. V. Teryaev, Sov. J. Nucl. Phys **36**, 140 (1982).
- [81] X. Ji, J. W. Qiu, W. Vogelsang, F. Yuan, Phys. Rev. Lett. **97**, 082002 (2006).
- [82] A. Adare *et al* (PHENIX), Phys. Rev. Lett. **103**, 012003 (2009); **93**, 202002 (2004).
- [83] B. I. Abelev *et al* (STAR), Phys. Rev. Lett. **100**, 232003 (2008).
- [84] J. C. Collins, Phys. Lett. B **536**, 43 (2002).